



## Effect of Microstructure, Chemical Composition, and Open Porosity on Oxidation Resistance of ZrB<sub>2</sub>-Based Composites

A. Hanifi<sup>a</sup>, Z. Balak<sup>a\*</sup><sup>a</sup> Department of Materials Science and Engineering, Ahvaz Branch, Islamic Azad University, Ahvaz, Khuzestan, Iran

## ARTICLE INFO

## ABSTRACT

## Article History:

Received 13 September 2020

Received in revised form 10 October 2020

Accepted 19 October 2020

## Keywords:

ZrB<sub>2</sub>-30 vol% SiC

Oxidation

HfB<sub>2</sub>

SPS

In this research, the effect of microstructure, chemical composition, and open porosity on the oxidation resistance of ZrB<sub>2</sub>-based composites was investigated. To this end, four composites with different chemical compositions were consolidated by Spark Plasma Sintering (SPS) method in different conditions, namely different temperature, time, and pressure. The open porosity was measured using the Archimedes method. Image Analysis Tools (IAT) were also utilized to determine the grain size of all composites through SEM images. For oxidation test, the samples were put on the box furnace and oxidized at 1400 C at different holding times of 20, 40, 60, and 120 minutes. The oxidation resistance was evaluated by weighing the samples before and after oxidation and the  $\Delta w$  was considered as the oxidation criterion. In addition, EDS analysis was used to identify the phases. The results showed that chemical composition was the most significant factor in terms of the oxidation resistance, least affected by open porosity. Sample 9, with a grain size of 2.5  $\mu\text{m}$  and open porosity of 1.5%, had the least oxidation value of 0.0026 gr; however, Sample 4 with a grain size of 12  $\mu\text{m}$  and open porosity of 0.68% had the highest oxidation value of 0.0176 gr.

<https://doi.org/10.30501/acp.2020.204582.1043>

## 1. INTRODUCTION

Zirconium diboride or ZrB<sub>2</sub> is one of the most investigated materials in the class of Ultra-High Temperature Ceramics (UHTCs) due to its interesting combination of physico-chemical and engineering properties, placing it among the most applicable compounds in the hottest parts of the next-generation aerospace vehicles [1,2].

Since the oxidation resistance is improved by making a composite with additives, ZrB<sub>2</sub> does not fully possess the oxidation resistance [3-6] required for surviving the re-entry conditions.

Numerous researchers have investigated the improvement of oxidation resistance of ZrB<sub>2</sub>-based ceramics [3-6]. Obviously, introduction of compounds containing Si- such as SiC, MoSi<sub>2</sub>, and WSi<sub>2</sub> would

enhance the oxidation resistance due to the formation of borosilicate layers on the outer surface of the ZrB<sub>2</sub> matrix which acts as the inhibitor of oxygen diffusion.

SiC, regarded among additives as the most effective one, was investigated in compositions with 5–50 vol.% of SiC for ZrB<sub>2</sub> in a wide range of test temperatures and pressures in which 20 vol.% compositions were regarded as optimal for hypersonic vehicles in a series of efforts supported by the US Air Force [4-6].

For a composition consisting of 80 vol% ZrB<sub>2</sub> and 20 vol% SiC at 1823 K, oxygen diffusivity in the borosilica was evaluated at  $1.7 \times 10^{-14}$  m<sup>2</sup>/s for a B<sub>2</sub>O<sub>3</sub>-21 mol% SiO<sub>2</sub> composition which was 10<sup>7</sup> times higher than that for pure silica, yet much lower than that for oxygen in ZrO<sub>2</sub> (~10<sup>-10</sup> m<sup>2</sup>/s at 1773 K). The refractory ZrB<sub>2</sub>-SiC system has an eutectic melting temperature of approximately 2573 K [6-10].

\* Corresponding Author Email: [zbalak1983@gmail.com](mailto:zbalak1983@gmail.com) (Z. Balak)URL: [https://www.acerp.ir/article\\_125792.html](https://www.acerp.ir/article_125792.html)

Please cite this article as: Hanifi, A., Balak, Z., "Effect of Microstructure, Chemical Composition, and Open Porosity on Oxidation Resistance of ZrB<sub>2</sub>-Based Composites", *Advanced Ceramics Progress*, Vol. 6, No. 4, (2020), 37-44



However, in a condition characterized by a relatively high temperature and low-oxygen partial pressure, SiC is oxidized in an active mode and its oxidation behaviors at ZrB<sub>2</sub>-SiC system are different from those in atmospheric air. Typically, Gao et al. [11] reported that in case the ZrB<sub>2</sub>-SiC ceramic was oxidized in low-pressure O<sub>2</sub>/N<sub>2</sub> mixture gas, ZrSiO<sub>4</sub> began to form at a temperature below 1600 °C. Moreover, they [12] reported that during the oxidation of ZrB<sub>2</sub>-SiC composite in low-pressure O<sub>2</sub>/N<sub>2</sub> mixture gas at 1500 °C, when the oxygen partial pressure decreased, the oxidation kinetics changed from the parabolic law to the linear law. Moreover, Jin et al. [13] reported the same change for ZrB<sub>2</sub>-SiC-Graphite composite when it was oxidized at 1800 °C in low-pressure O<sub>2</sub>/Ar mixture gases.

Zapata-Solvas studied the effect of introducing La<sub>2</sub>O<sub>3</sub> on the oxidation resistance of ZrB<sub>2</sub>-20 vol% SiC in the temperature range of 1400–1600 °C [14]. Of note, in this temperature range, the ZrB<sub>2</sub>-20 vol% SiC composites exhibited kinetics of mass gain following a power law ( $\Delta w = kt^n$ ) where  $1 \leq n \leq 2$ , implying that oxidation rates were to be intermediate between those expected from linear and parabolic kinetics; however, introduction of La<sub>2</sub>O<sub>3</sub> to the composite would lead to the kinetics based on the parabolic rate law, thus improving the oxidation resistance.

Other researchers have investigated the oxidation behaviors of a ZrB<sub>2</sub>-SiC-La<sub>2</sub>O<sub>3</sub>/SiC dual-layer coating on the siliconized graphite at 1800 °C under low air pressures. In oxidation kinetics, a transition of the coated samples from parabolic weight gain to linear weight loss with a decrease in the air pressure was observed. A protective oxide scale comprising ZrO<sub>2</sub> and SiO<sub>2</sub> with La dispersed was formed on the coating surface after oxidation in 50 kPa air [15].

The kinetics and oxide scale evolution during isothermal exposure of ZrB<sub>2</sub>-20 SiC-LaB<sub>6</sub> composites sintered by spark-plasma at 1300 °C in different time periods were examined. The variation of mass gain with time was expressed by near-parabolic rate law during a time period of 0–8 h and by the relations that were suggestive of slower kinetics within 8–24 h, with parabolic rate constants ( $k_p$ ) decreasing sharply [16].

Introducing LaB<sub>6</sub> to ZrB<sub>2</sub>-SiC composites would contribute to the oxidation resistance by forming a refractory La<sub>2</sub>Zr<sub>2</sub>O<sub>7</sub> and/or La<sub>2</sub>Si<sub>2</sub>O<sub>7</sub> scale on the outermost surface of oxide scale [17-19].

In our previous study [20], the effect of both different additives, namely SiC, C<sub>f</sub>, MoSi<sub>2</sub>, ZrC, and HfB<sub>2</sub>, and SPS conditions, including temperature, time, and pressure, were studied using Taguchi design; in addition, the effect of each variable and its incorporation on the oxidation resistance was determined. In the present study, different compositions and SPS conditions were selected to investigate the effect of microstructure, chemical composition, and open porosity on the oxidation resistance of ZrB<sub>2</sub>-based composites.

## 2. MATERIALS AND METHODS

ZrB<sub>2</sub>, SiC, ZrC, C<sub>f</sub>, MoSi<sub>2</sub>, and HfB<sub>2</sub> powders were used as the raw materials. Four composites with different compositions were consolidated by SPS method under different sintering conditions according to Table 1. First, the weighed powders were ball-milled using zirconia balls through ethanol as milling media in a zirconia cup. The details were expressed elsewhere [12-14]. The process of sintering through spark plasma method was then carried out via SPS furnace (SPS-20T-10: china) in different conditions based on Table 1. To remove the remaining graphite foil, the obtained disk-shaped samples were grinded and then, wire cut to achieve 2×4×10 mm beam-shaped samples for oxidation test. The oxidation test was performed in a box furnace at 1400°C for 20, 40, 60, and 120 min. The weight change was then measured as the oxidation progress criterion, according to the following equation [4-6]:

$$\Delta W_{C-O} \% = \frac{W_i - W_a}{W_i} \times 100 \quad (1)$$

where  $W_{C-O}$  shows the percentage of weight change due to oxidation, and  $W_i$  and  $W_a$  present the initial and after-oxidation weights of the samples, respectively.

**TABLE 1.** Compositions and SPS conditions of four composites

Sample	Factor.1	Factor.2	Factor.3	Factor.4	Factor.5	Factor.6	Factor.7	Factor.8	Factor.9
	SiC Vol%	C <sub>f</sub> Vol%	(M.t)	MoSi <sub>2</sub> Vol%	HfB <sub>2</sub> Vol%	ZrC Vol%	Tem. C	Press. MPa	Time min
4	5	7.5	7.5	6	15	15	1900	40	16
7	10	5	5	6	15	0	1600	20	8
9	15	0	2.5	4	15	0	1700	30	16
13	20	0	2.5	6	10	10	1900	20	4

## 3. RESULTS AND DISCUSSION

### 3.1. MICROSTRUCTURAL INVESTIGATION

In order to survey the composite microstructure, SEM images of these four composites were employed, as presented in Fig. 1. According to the previous research [21-23], the black grains are SiC and the dark gray grains are pure ZrB<sub>2</sub>. The light phases shown in Composite 7 are HfB<sub>2</sub> and finally, the approximately light phases are (Zr, Hf)B<sub>2</sub> solid solution or ZrC. These approximately light phases can be observed more frequently in Composite 7 rather than Composite 4. Moreover, pure HfB<sub>2</sub> (light phase) is not observed in Composite 4. Such differences are observed mainly due to the Hf diffusion to Zr lattice. Based on SPS parameters such as higher temperature, time, and pressure, it can be concluded that diffusion conditions are more supported in Composite 4 than in

Composite 7. In other words, because of the mentioned parameters, the required situation for Hf diffusion and full solution are supported; thus, no pure  $\text{HfB}_2$  can be observed.

A comparison of the SEM images shown in Fig. 1 showed that Composite 7 had higher porosity than others. For more investigation, the percentage of open porosity of composites and their grain sizes are given in Table 2. While Composites 4 and 13 had the least open porosity due to the high sintering temperature of  $1900^\circ\text{C}$ , Composite 7 had the highest open porosity due to the low sintering temperature of  $1600^\circ\text{C}$ .

Compared to Composites 7, 9, and 13, Composite 4 had the largest grain size mainly due to the high temperature and time of SPS and low amount of SiC functioning as the grain growth inhibitor. Fine grain microstructure in Composites 7 and 9 was obtained as a result of lower sintering temperatures of  $1600$  and  $1700^\circ\text{C}$  and higher SiC additive. Although Composite 13 was consolidated at a high sintering temperature of  $1900^\circ\text{C}$ , it had a fine grain size owing to the higher amount of SiC.

To investigate the oxidation resistance and determine the phase formation in composites, the SEM images of cross-sections and their map analysis were employed, as shown in Fig. 2.

Fig. 2 shows the SEM images of the cross-section of Composite 4 after oxidation at  $1400^\circ\text{C}$  at different times. While for Samples 4-20, 4-40, and 4-60, the microstructure of the cross-section contains a black layer with elongated white grains (needle grains), in Sample 4-120, this layer was not found. To identify the phases, both point and map were analyzed, as shown in Figs. 3 and 4. According to the analysis of the points A and B in Fig. 3, this black layer is  $\text{SiO}_2$  and the white grains are  $\text{HfO}_2$  and  $\text{ZrO}_2$ . A comparison of the SEM images in Fig. 2 revealed that the microstructure coarsened with oxidation time. Furthermore, it was observed that the number of white grains in the black layer of  $\text{SiO}_2$  decreased and the thickness of the oxide layer increased. Reduction of white grains of  $\text{ZrO}_2$  and  $\text{HfO}_2$  would be indicative of the oxidation resistance with time. Furthermore, an analysis of the map images in Fig. 4 showed the depleted C/Si layer with high thickness, suggesting that in the process of exposing the sample at oxidation atmosphere at  $1400$  temperature, the oxidation was noticeable.

TABLE 2. Open porosity and grain size of all samples

Sample	Average Open porosity %	Grain Size $\mu\text{m}$
4	0.68	12
7	12.8	2
9	1.1	2.5
13	1.15	3.5

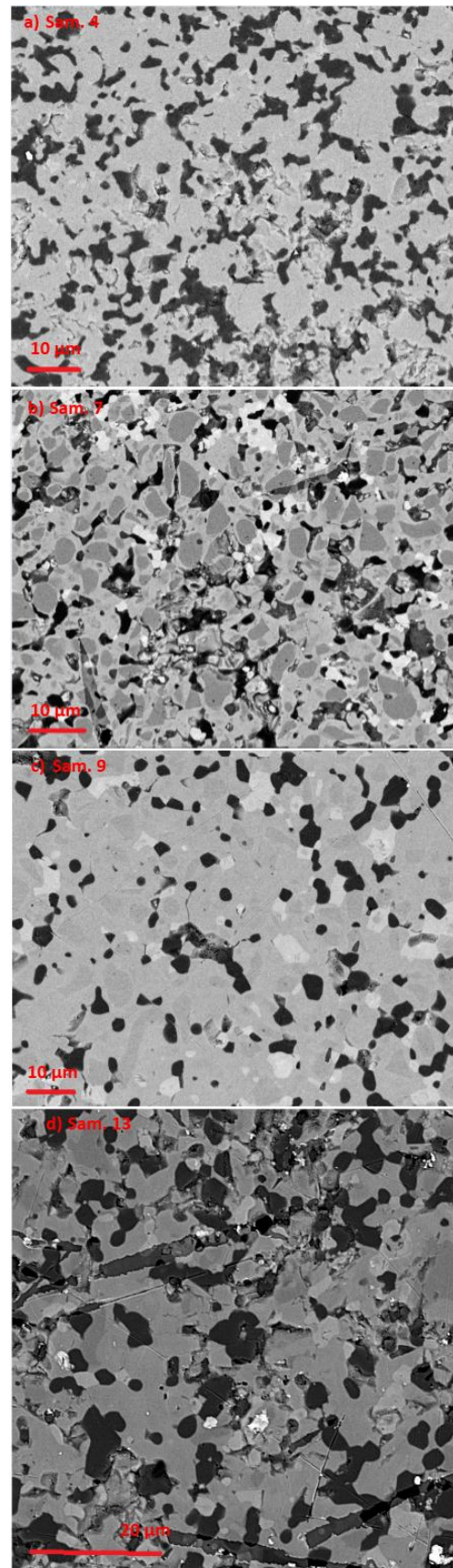
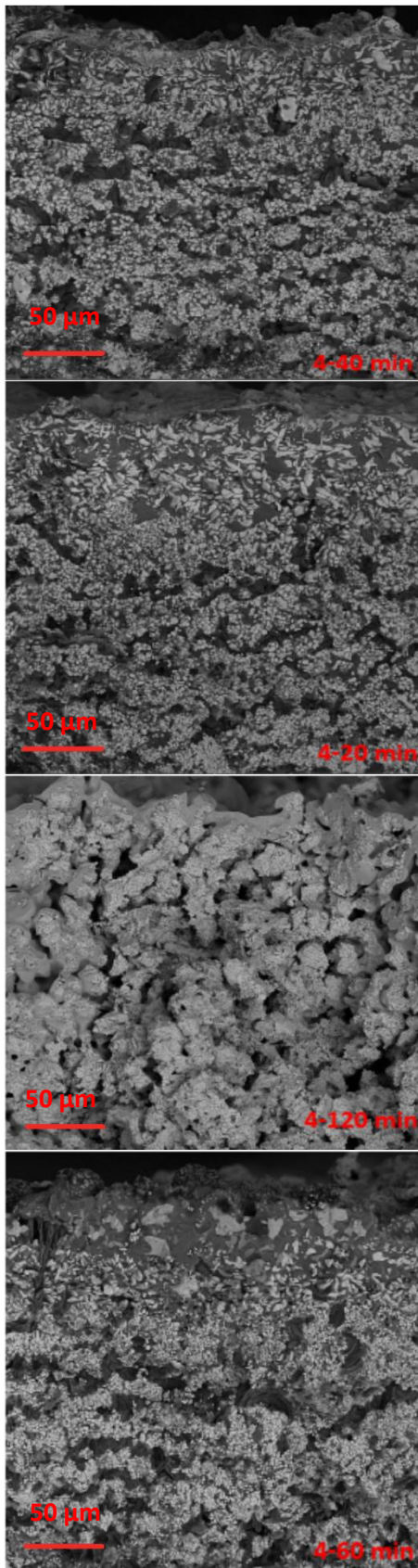
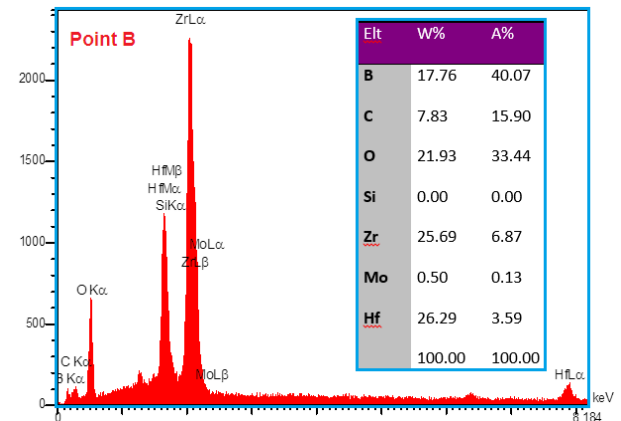
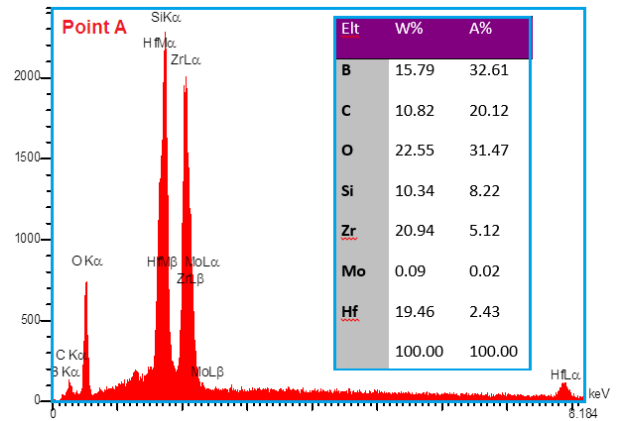
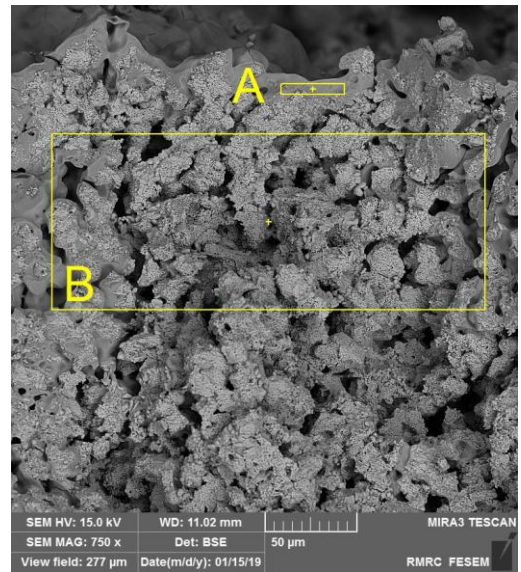


Figure 1. SEM images of samples a) 4, b) 7, c) 9, and d) 13





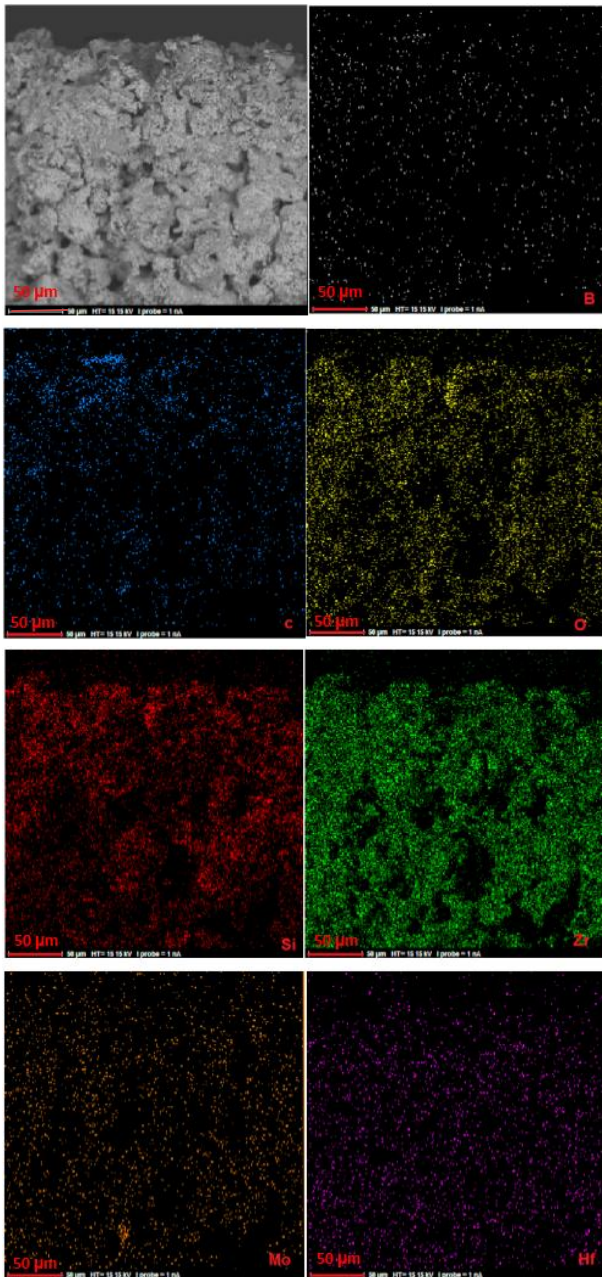
**Figure 2.** SEM images of the cross-section of Sample 4 after oxidation at 1400 °C for different times



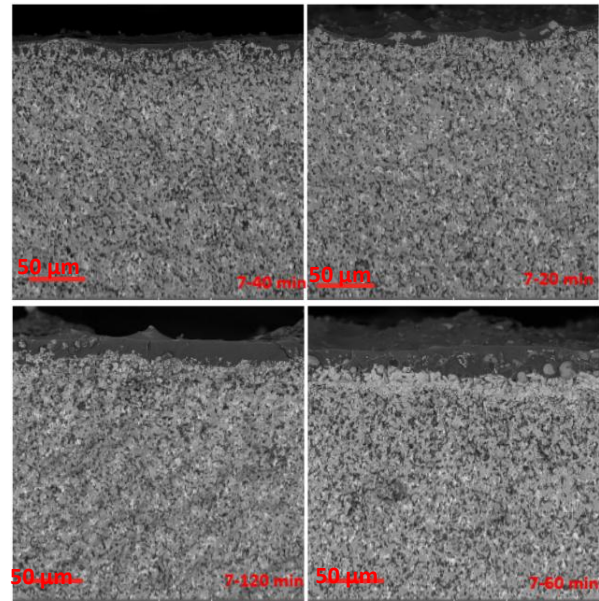
**Figure 3.** SEM images and point analysis of Sample 4 after oxidation at 1400 C for 120 min

Fig. 5 presents the SEM images of Sample 7 after oxidation at 1400 °C for different times. Obviously, thickness of the affected zone (oxide zone) increased with oxidation time. Moreover, according to the point

analysis in Fig. 6, the sample surface comprised elements such as O, B, and Si, indicating that this layer was a combination of  $\text{SiO}_2$  and  $\text{B}_2\text{O}_3$  (point A). While at points B and C, the amount of  $\text{SiO}_2$  and  $\text{B}_2\text{O}_3$  decreased noticeably, that of Zr and Hf increased Fig. 7 depicts the SEM images of Samples 9 and 13 at two magnifications after oxidation at 1400 °C for 2 hours. Similar to Samples 4 and 7, the cross-section of Sample 9 contains a  $\text{SiO}_2$  black layer with white  $\text{ZrO}_2$  grains.



**Figure 4.** SEM images and map analysis of Sample 4 after oxidation at 1400 C for 120 min

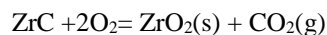


**Figure 5.** SEM images of cross-section of Sample 7 after oxidation at 1400 C for different times

### 3.2. OXIDATION RESISTANCE

The SEM images of all samples after oxidation at 1400 °C for 2 hr as well as the thickness of the oxide layer are given in Figs. 9 and 10.

As observed, the microstructure of Sample 4 was different from others that contained more coarse grains and porosities. Coarse grains originated from sintering conditions. Coarse porosities were formed as a result of consumed elements such as Zr, Si, and Hf in  $\text{ZrC}$ ,  $\text{ZrB}_2$ ,  $\text{SiC}$ , and  $\text{HfB}_2$ . In fact, the pure  $\text{ZrB}_2$  is oxidized at 1100 °C and creates  $\text{B}_2\text{O}_3$  which evaporates at 1400 °C.  $\text{SiC}$  reacts with  $\text{B}_2\text{O}_3$  and produces a  $\text{SiO}_2$ - $\text{B}_2\text{O}_3$  glassy layer. Since  $\text{SiC}$  amount is low (5 vol%) in this composite, during a two-hour exposure in the oxidation environment at 1400 °C,  $\text{B}_2\text{O}_3$  evaporates and induces porosities in microstructure. Moreover, the very poor oxidation resistance of  $\text{ZrC}$  (380 °C), according to the following reaction, promotes porosity formation.



According to Fig. 11, with an increase in the oxidation time,  $\Delta w$  increases which is in total agreement with the thickness of the oxidation layer increment (Figs. 2, 5, 7, and 8).

$\Delta w$  occurs as a result of greater oxygen diffusion. According to the SEM images of Fig. 9 and oxidation curves in Fig. 11, Sample 9 exhibits different weights vs. oxidation time. Fig. 11 shows a comparison between oxidation values of all samples at different oxidation times.

Among all samples, Samples 7, 13, and 14 exhibited the highest oxidation resistance. Typically, the following factors justify the higher oxidation resistance of Sample 9 than Sample 4: A) larger microstructure grain size in



Sample 9 due to lower sintering temperature (1700 °C) than sample 4 (1900 °C) and higher amount of SiC as grain growth inhibitor (15 Vol% to 5 Vol%5), leading to positive effects on oxidation resistance; (B) chemical composition, according to previous research [21-23], in which SiC reacts with oxygen and creates adhesive SiO<sub>2</sub> layer which noticeably improves the oxidation resistance of ZrB<sub>2</sub>-based ceramics.

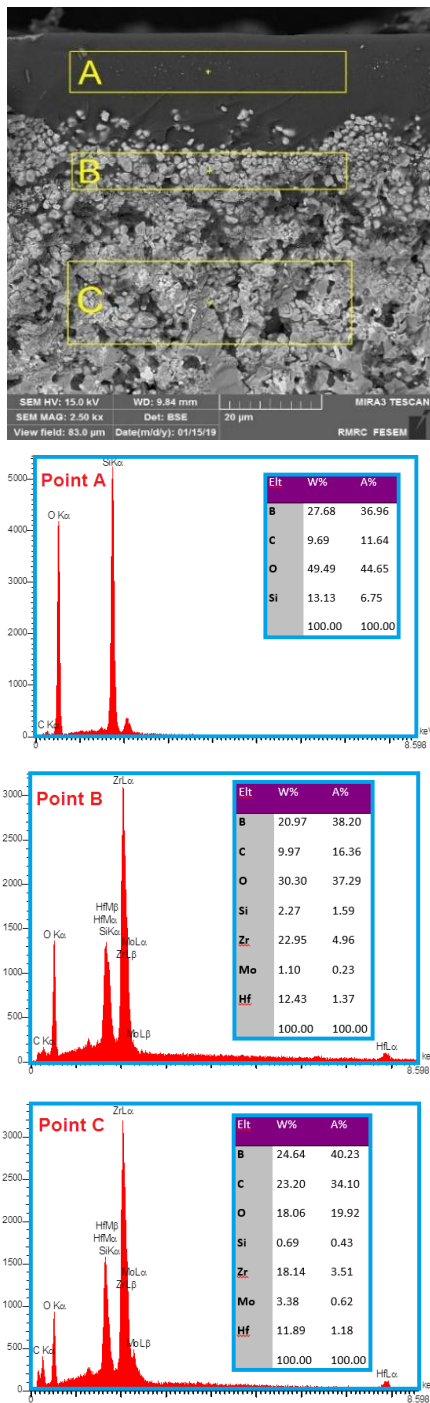


Figure 6. SEM image and point analysis of Sample 7

Sample 9 contains a greater amount of SiC than Sample 4, hence better oxidation resistance. Moreover, the carbon fiber, whose amount is higher in Sample 4, has detrimental effect on the oxidation resistance [21]. Finally, other research has shown that the ZrC is oxidized at low temperatures (nearly 600 °C) and its high amount (15 vol%) in Sample 4 resulted in reducing its oxidation resistance rather than Sample 9. Totally, it can be concluded that both the finer microstructure and the desired chemical composition in Sample 9 caused higher oxidation resistance than Sample 4. Open porosity percentage can be an effective factor in oxidation resistance.

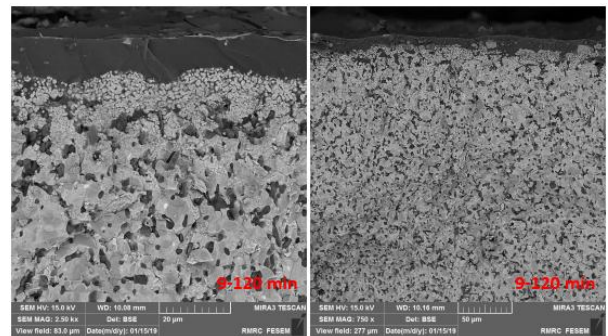


Figure 7. SEM images of the cross-section of Sample 9 after oxidation at 1400 °C for 120 min at two magnifications

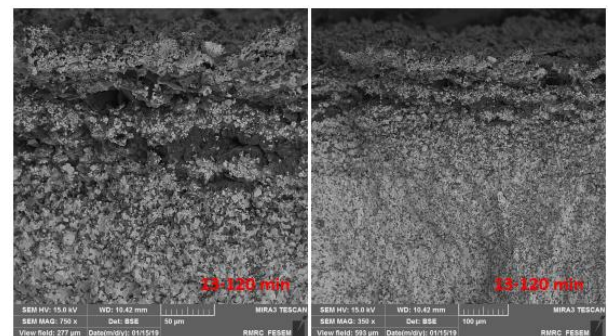


Figure 8. SEM images of the cross-section of Sample 13 after oxidation at 1400 °C for 120 min at two magnifications

Samples 7 and 9 with almost the same chemical compositions and grain sizes were selected for further study. According to Fig. 11, the oxidation resistance of Sample 7 is lower probably due to its higher open porosity, presented in Table 1. Therefore, open porosity by supporting the paths for oxygen diffusion could considerably promote oxygen diffusion to the substrate and reduce the oxidation resistance. Of note, open porosity had the less effect than grain size and chemical composition.

In other words, lower oxidation resistance of Samples 4-13 could be attributed to the coarse grain size, lower SiC, and presence of carbon fiber.

A comparison of Samples 7 and 13 showed that although Sample 7 had higher open porosity, its oxidation resistance was better. With respect to their grain size and

chemical composition, it is clear that both of them have the same grain size with different chemical compositions. Thus, it can be concluded that the chemical composition of Sample 7 is desirable in reaching higher oxidation resistance.

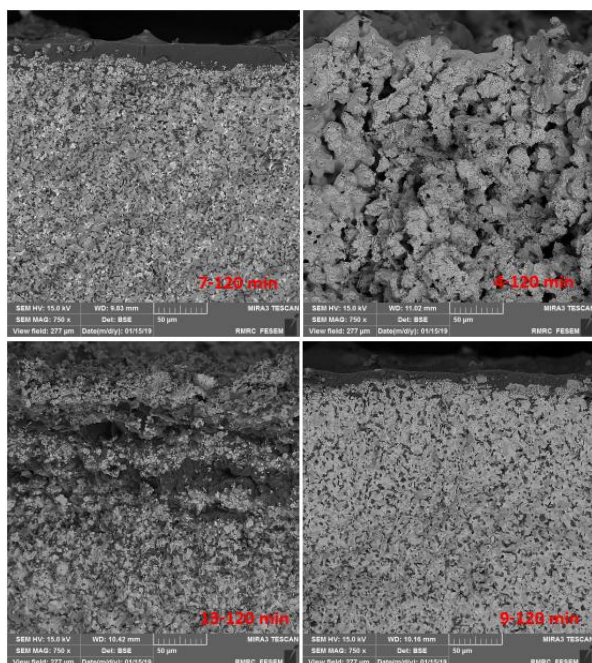


**Figure 9.** SEM images of the cross-section of all samples after oxidation at 1400°C for 120 min

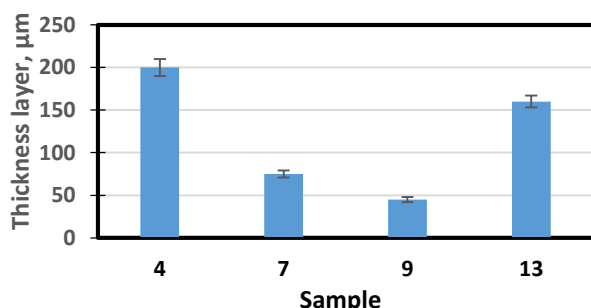


**Figure 10.** Thickness of the oxide layer of all samples after oxidation at 1400 °C for 120 min

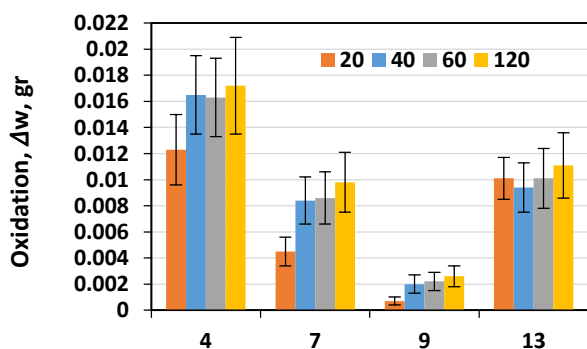


**Figure 11.** Comparison of weight change of all samples after oxidation at 1400 °C at different times

## 4. CONCLUSIONS

- 1- Based on the findings in this study, it can be concluded that factors such as chemical compositions, grain size, and open porosity could considerably affect oxidation resistance, among which chemical composition and open porosity had the most and the least effects, respectively.
- 2- Among different additives, SiC could significantly improve the oxidation resistance.
- 3- ZrC and carbon fiber had detrimental effect on the oxidation resistance.
- 4- During the oxidation at 1400 C,  $\text{ZrO}_2$ ,  $\text{SiO}_2$ , and  $\text{HfO}_2$  phases were formed.
- 5- The best oxidation resistance (0.0026 gr ) was obtained for Composite 9 ( $\text{ZrB}_2$ -15SiC-15HfB<sub>2</sub>-4MoSi<sub>2</sub>) due to its combination of desirable chemical composition and microstructure (low open porosity and fine grain size).
- 6- The worst oxidation resistance (0.0176 gr ) was obtained for Composite 4 ( $\text{ZrB}_2$ -15ZrC-15HfB<sub>2</sub>-7.5C<sub>f</sub>-6MoSi<sub>2</sub>-5SiC) due to its coarse grain size, low SiC amount, and presence of ZrC.

## ACKNOWLEDGEMENT

This article has been extracted from the research project in the name of " Investigation of oxidation mechanism of  $\text{ZrB}_2$ -SiC based composites" which was supported by Islamic Azad University of Ahvaz.

## REFERENCES

1. Asl, M.S., Kakroudi, M.G., Nayebi, B., Nasiri, H., "Taguchi analysis on the effect of hot pressing parameters on density and hardness of zirconium diboride", *International Journal of Refractory Metals and Hard Materials*, Vol. 50, (2015), 313-320. <https://doi.org/10.1016/j.jrmhm.2014.09.006>
2. George, M. R., "Studies of ultra-high temperature ceramic composite components: synthesis and characterization of  $\text{HfO}_x\text{C}_y$  and Si oxidation in atomic oxygen containing environments", P.H.D Thesis, *Vander Bilt university*, 2008.
3. Guo, W. M., Zhang, G. J., "Oxidation resistance and strength retention of  $\text{ZrB}_2$ -SiC ceramics", *Journal of the European Ceramic Society*, Vol. 30, No. 11, (2010), 2387-2395. <https://doi.org/10.1016/j.jeurceramsoc.2010.01.028>
4. Sarin, P., Driemeyer, P.E., Haggerty, R.P., Kim, D. K., Bell, J.L., Apostolov, Z.D., Kriven, W.M., "In situ studies of oxidation of  $\text{ZrB}_2$  and  $\text{ZrB}_2$ -SiC composites at high temperatures", *Journal of the European Ceramic Society*, V. 30, No. 11, (2010), 2375-2386. <https://doi.org/10.1016/j.jeurceramsoc.2010.03.009>
5. Rezaie, A. R., , Fahrenholtz, W. G., Hilmars, G. E., "The effect of a graphite addition on oxidation of  $\text{ZrB}_2$ -SiC in air at 1500 °C", *Journal of the European Ceramic Society*, Vol. 33, No. 2, (2013), 413-421. <https://doi.org/10.1016/j.jeurceramsoc.2012.09.016>

6. Han, J., Hu, P., Zhang, X., Meng, S., Han, W., "Oxidation-resistant ZrB<sub>2</sub>-SiC composites at 2200 °C", *Composites Science and Technology*, Vol. 68, No. 3-4, (2008), 799–806. <https://doi.org/10.1016/j.compscitech.2007.08.017>
7. Rezaie, A., Fahrenholtz, W.G., Hiltmas, G.E., "Evolution of structure during the oxidation of zirconium diboride-silicon carbide in air up to 1500 °C", *Journal of the European Ceramic Society*, Vol. 27, No. 6, (2007), 2495–501. <https://doi.org/10.1016/j.jeurceramsoc.2006.10.012>
8. Fahrenholtz, W.G., "Thermodynamic analysis of ZrB<sub>2</sub>-SiC oxidation: formation of a SiC-depleted region", *Journal of the American Ceramic Society*, Vol. 90, No. 1, (2007), 143–148. <https://doi.org/10.1111/j.1551-2916.2006.01329.x>
9. Williams, P.A., Sakidja, R., Perepezko, J.H., Ritt, P., "Oxidation of ZrB<sub>2</sub>-SiC ultra-high temperature composites over a wide range of SiC content", *Journal of the European Ceramic Society*, Vol. 32, No. 14, (2012), 3875–3883. <https://doi.org/10.1016/j.jeurceramsoc.2012.05.021>
10. Liu, H. L., Liu, J. X., Liu, H.T., Zhang, G.J., "Changed oxidation behavior of ZrB<sub>2</sub>-SiC ceramics with the addition of ZrC", *Ceramics International*, Vol. 41, No. 6, (2015), 8247–8251. <https://doi.org/10.1016/j.ceramint.2015.02.150>
11. Gao, D., Zhang, Y., Fu, J.Y., Xu, C.L., Song, Y., Shi, X.B., "Oxidation of zirconium diboride-silicon carbide ceramics under an oxygen partial pressure of 200 Pa: formation of zircon", *Corrosion science*, Vol. 52, No. 10, (2010), 3297–3303. <https://doi.org/10.1016/j.corsci.2010.06.004>
12. Tian, C.Y., Gao, D., Zhang, Y., Fu, J.Y., Xu, C.L., Song, Y., Shi, X.B., "Oxidation behaviour of zirconium diboride-silicon carbide ceramic composites under low oxygen partial pressure", *Corrosion science*, Vol. 53, No. 11, (2011) 3742–3746. <https://doi.org/10.1016/j.corsci.2011.07.020>
13. Jin, H., Meng, S., Xinghong, Z., Qingxuan, Z., Weihua, X., "Oxidation of ZrB<sub>2</sub>-SiC-graphite composites under low oxygen partial pressures of 500 and 1500 Pa at 1800 °C", *Journal of the American Ceramic Society*, Vol. 99, No. 7, (2016), 2474–2480. <https://doi.org/10.1111/jace.14232>
14. Zapata-Solvas, E., Jayaseelan, D.D., Brown, P.M., Lee, W.E., "Effect of La<sub>2</sub>O<sub>3</sub> addition on long-term oxidation kinetics of ZrB<sub>2</sub>-SiC and HfB<sub>2</sub>-SiC ultra-high temperature ceramics", *Journal of the European Ceramic Society*, Vol. 34, No. 15, (2014), 3535–3548. <https://doi.org/10.1016/j.jeurceramsoc.2014.06.004>
15. Rena, Y., Qian, Y., Xu, J., Zuo, J., Li, M., "Oxidation resistance and microstructure evolution of ZrB<sub>2</sub>-SiC-La<sub>2</sub>O<sub>3</sub>/SiC dual-layer coating on siliconized graphite at 1800 °C under low air pressures", *Ceramics International*, Vol. 46, No. 17, (2020), 27150–27157. <https://doi.org/10.1016/j.ceramint.2020.07.195>
16. Kashyap, S.K., Kumar, A., Mitra, R., "Kinetics and evolution of oxide scale during various stages of isothermal oxidation at 1300 °C in spark plasma sintered ZrB<sub>2</sub> - SiC - LaB<sub>6</sub> composites", *Journal of the European Ceramic Society*, Vol. 40, No. 15, (2020), 4997–5011. <https://doi.org/10.1016/j.jeurceramsoc.2020.07.053>
17. Zhang, X.H., Hu, P., Han, J.C., Xu, L., Meng, S.H., "The addition of lanthanum hexaboride to zirconium diboride for improved oxidation resistance", *Scripta Materialia*, Vol. 57, No. 11, (2007), 1036–1039. <https://doi.org/10.1016/j.scriptamat.2007.07.036>
18. Jayaseelan, D.D., Zapata-Solvas, E., Brown, P., Lee, W.E., "In situ formation of oxidation resistant refractory coatings on SiC-reinforced ZrB<sub>2</sub> ultra high temperature ceramics", *Journal of the American Ceramic Society*, Vol. 95, No. 4, (2012), 1247–1254. <https://doi.org/10.1111/j.1551-2916.2011.05032.x>
19. Hu, P., Zhang, X.H., Han, J.C., Luo, X.G., Du, S.Y., "Effect of various additives on the oxidation behavior of ZrB<sub>2</sub>-based ultra-high-temperature ceramics at 1800°C", *Journal of the American Ceramic Society*, Vol. 93, No. 2, (2010) 345–349. <https://doi.org/10.1111/j.1551-2916.2009.03420.x>
20. Balak, Z., Azizieh, M., "Oxidation of ZrB<sub>2</sub>-SiC composites at 1600 °C: Effect of carbides, borides, silicides, and chopped carbon fiber", *Advanced Ceramics Progress*, Vol. 4, No. 1, (2018), 18–23. <https://dx.doi.org/10.30501/acp.2018.90829>
21. Balak, Z., Zakeri, M., Rahimpour, M., Salahi, E., "Taguchi design and hardness optimization of ZrB<sub>2</sub>-based composites reinforced with chopped carbon fiber and different additives and prepared by SPS", *Journal of Alloys and Compounds*, Vol. 639, (2015), 617–625. <https://doi.org/10.1016/j.jallcom.2015.03.131>
22. Balak, Z., Zakeri, M., "Application of Taguchi L<sub>32</sub> orthogonal design to optimize flexural strength of ZrB<sub>2</sub>-based composites prepared by spark plasma sintering", *International Journal of Refractory Metals and Hard Materials*, Vol. 55, (2016), 58–67. <https://doi.org/10.1016/j.ijrmhm.2015.11.009>
23. Balak, Z., Zakeri, M., Rahimpour, M.R., Salahi, E., Azizieh, M., Kafashan, H., "Investigation of Effective Parameters on Densification of ZrB<sub>2</sub>-SiC Based Composites Using Taguchi Method", *Advanced Ceramics Progress*, Vol. 2, No. 2, (2016), 7–15. <https://dx.doi.org/10.30501/acp.2016.90835>